Simulation of Intermodulation Distortion in Passive CMOS FET Mixers

Himanshu Khatri #, Prasad S. Gudem *, and Lawrence E. Larson #

#University of California San Diego, La Jolla, CA, 92093, USA
*Qualcomm Inc., San Diego, CA, 92121, USA

***Abstract*— The simulation of third-order intermodulation distortion in a passive CMOS FET mixer will typically predict a fictitious 2:1 slope using the industry standard EKV, BSIM3 and BSIM4 models. This phenomenon has been attributed to the discontinuity in the second-order derivatives of the drain-current and the terminal charge model. This paper establishes the connection between the discontinuous derivatives and the resulting intermodulation distortion slope and provides experimental verification.**

***Index Terms*— Passive mixer, Semiconductor device modeling, BSIM, EKV, PSP, Gummel symmetry.**

I. Introduction

Passive CMOS mixers have gained wide popularity in modern integrated receiver systems, owing to better voltage headroom, flicker noise and negligible power consumption as compared to active implementations. Several detailed studies have been undertaken to address passive mixer design concerns, such as noise, dc offset, and second-order distortion [1]–[3]. However, little detailed analysis has been published on the third-order nonlinear behavior of these mixers. With a motivation of eliminating the off-chip RF filter, it is important to pay close attention to the mixer nonlinearity and to obtain an accurate simulation estimate of the mixer nonlinearity.

At the V_{DS}=0 bias, the BSIM3v3, BSIM4, Philips MM9 and EKV models deviate from the measured results, due to discontinuities in the higher order derivatives of drain current and terminal charges [4]–[8]. These models typically predict an anomalous IM_3 slope of 2:1, instead of 3:1, for the third-order intermodulation distortion in a passive mixer. Nevertheless, these models still meet the Gummel symmetry condition, i.e., the drain current is a symmetric function of V_{DS}, when V_D+V_S is kept constant. This paper aims at explaining the mechanism through which the discontinuity in the second derivative of the drain current leads to a 2:1 slope for the third-order distortion, and provide precise guidelines for minimizing anomalous IM_3 behavior in passive mixer simulation.

The latest surface-potential based model, PSP [9] and the next generation BSIM model, BSIM5 [10], [11] have overcome this limitation and give the correct slope of 3:1 for the third-order distortion.

II. CMOS I_D versus V_{DS} Relationship

For a MOS transistor, the typical Gummel symmetry test is conducted by exciting the source and drain terminals with equal and opposite voltages (odd mode excitation). In this scenario, the drain current, I_D can be expressed as a polynomial function of the drain-source voltage, V_{DS}, as,

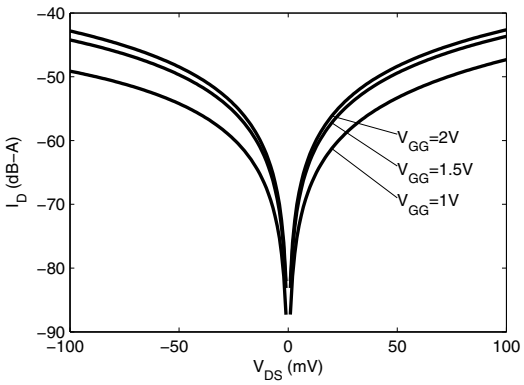

Fig. 1. Simulated I_D versus V_{DS} curve for a 50 μm/0.18 μm NMOS transistor using BSIM3v3 model. $V_D + V_S = 0$, V_{GG} = gate voltage.

$$I_D = a_1 V_{DS} + a_2 V_{DS}^2 + a_3 V_{DS}^3 + a_4 V_{DS}^4 + \dots \quad (1)$$

The simulated drain current using the BSIM3v3 model for different gate voltages is shown in Fig. 1. Evidently, the model correctly exhibits Gummel symmetry, hence, it is required that,

$$I_D(V_{DS}) = -I_D(-V_{DS}) \quad (2)$$

This is possible when the even-order coefficients (a_2, a_4, etc) in (1) are either zero or are equal and opposite in sign for positive and negative values of V_{DS}. In the newer generation models (PSP, BSIM5), these even-order coefficients are zero, while in the earlier models these are discontinuous at $V_{DS} = 0$ and have equal and opposite values in the two regions. For these later cases, the drain current should be expressed as a piecewise polynomial function of the drain-source voltage as shown in (3), i.e.

$$I_D = \begin{cases} a_1 V_{DS} + a_2 V_{DS}^2 + a_3 V_{DS}^3 + \dots & \text{for } V_{DS} > 0 \\ a_1' V_{DS} + a_2' V_{DS}^2 + a_3' V_{DS}^3 - \dots & \text{for } V_{DS} < 0 \end{cases} \quad (3)$$

For maintaining the Gummel symmetry,

$$a_n' = \begin{cases} a_n & \text{for odd } n, \\ -a_n & \text{for even } n. \end{cases} \quad (4)$$

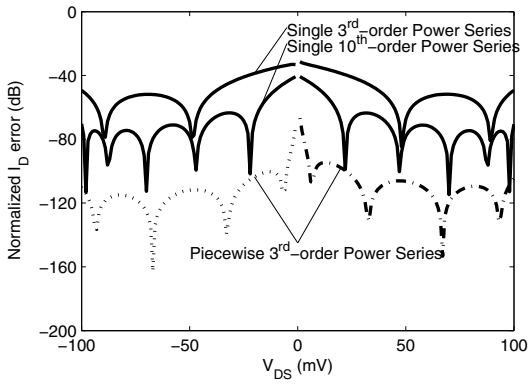

Fig. 2. Normalized mean square error in I_D estimation of Fig. 1, obtained using BSIM3v3 model, for a single third-order polynomial and a pair of piecewise polynomials.

The advantage of this piecewise representation can be shown by comparing the DC I_D simulation response to its polynomial estimations. Fig. 2 shows the normalized error in I_D estimation using third-order and tenth-order polynomials for the entire V_{DS} range ($\pm$100 mV). The third-order piecewise representation provides roughly 40 dB better estimation compared to a single power series representation of a much higher order.

III. Effect on Passive Mixer Linearity Simulation

Fig. 3(a) depicts a block diagram of a zero IF (ZIF) receiver. The low noise amplifier (LNA) acts as a transconductance stage and feeds the current to a current-commutating passive mixer. As we are concerned only with the mixer, Fig. 3(a) can be further simplified to Fig. 3(b) by replacing the LNA model with a current source i_{rf} and a shunt impedance, Z_S, and the TIA input with an impedance Z_L.

The primary sources of nonlinearity in a passive CMOS mixer driven by a square wave LO are the

– non-zero rise and fall time of the LO,

– nonlinear C_{gs} and C_{gd},

– and the nonlinear I_D versus V_{DS} relationship.

At lower microwave frequencies, a square-wave LO can be faithfully achieved in an IC environment and hence, the contributions from the finite rise time and nonlinear capacitances are negligible for short gate length devices. Hence, the mixer nonlinearity is dominated by the nonlinear $I_D - V_{DS}$ relation. The mixer operation can be analyzed by expressing the mixer input and the output voltages as weakly nonlinear power series expanded about the periodically varying LO voltage [12]. The coefficients of the ensuing series are time-varying; however, for a low-frequency operation, the memory elements in the mixer and the load impedance can be ignored and the coefficients are assumed to be constants. Hence, the mixer linearity can be estimated from the simplified circuit of Fig. 3(d). The load impedance, Z_L, for a current commutating mixer is typically low due to the feedback of the baseband transimpedance amplifier (TIA), while the mixer source impedance, Z_S, at the LNA output is relatively high.

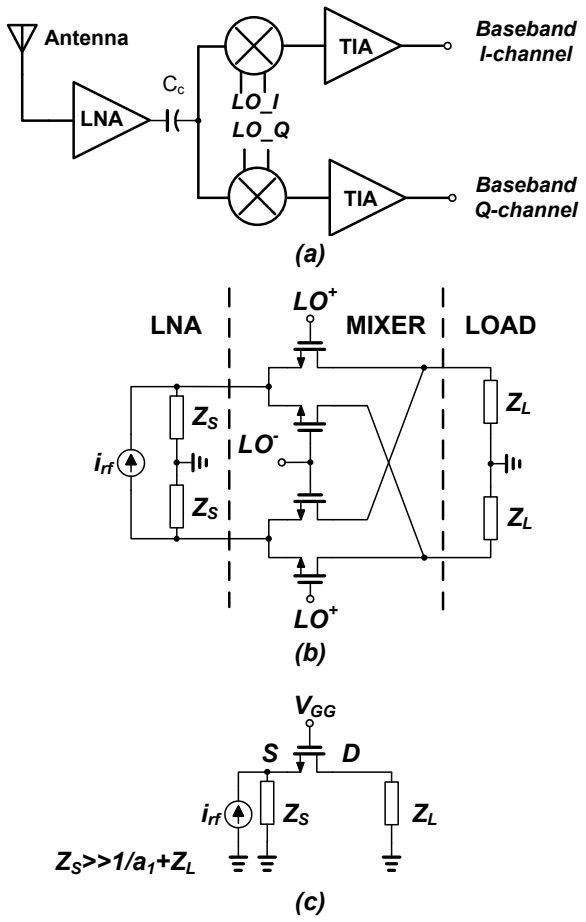

Fig. 3. (a) Receiver block diagram, (c) Passive Mixer model, (d) Mixer MOS transistor model.

For a two-tone intermodulation test, the current source can be expressed as,

$$i_{rf}(t) = A\cos(\omega_0 - \Delta\omega)t + A\cos(\omega_0 + \Delta\omega)t \qquad (5)$$

As discussed in the previous section, for the MOSFET models that exhibit discontinuous even-order coefficient at $V_{DS} = 0$, the output voltage should be expressed as,

$$V_D(t) = \begin{cases} b_1 i_{rf}(t) + b_2 i_{rf}^2(t) + b_3 i_{rf}^3(t) & \text{if } V_{DS}(t) < 0, \\ b_1' i_{rf}(t) + b_2' i_{rf}^2(t) + b_3' i_{rf}^3(t) & \text{if } V_{DS}(t) \geq 0, \end{cases} \qquad (6)$$

where, b_n and b_n' are constants dependent upon the transistor DC characteristics and the source and the load impedances. Assuming a high mixer linearity and assuming that the source impedance is much greater than $1/g_1$ and the load impedance combined, we can approximate $V_{DS}(t)$ as,

$$V_{DS}(t) \approx -\frac{i_{rf}(t)}{a_1}. \qquad (7)$$

Hence, (6) can be rewritten as,

$$V_D(t) \approx \begin{cases} b_1 i_{rf}(t) + b_2 i_{rf}^2(t) + b_3 i_{rf}^3(t) & \text{if } i_{rf}(t) > 0, \\ b_1' i_{rf}(t) + b_2' i_{rf}^2(t) + b_3' i_{rf}^3(t) & \text{if } i_{rf}(t) \leq 0. \end{cases} \qquad (8)$$

In this analysis, we find the fundamental and third-order intermodulation term of $V_D(t)$ by obtaining the contributions when $i_{rf}(t) > 0$ and $i_{rf}(t) < 0$ separately, and, then adding these contributions. We define the contribution from the positive half as,

$$V_D^+(t) = \begin{cases} V_D(t) & \text{if } i_{rf}(t) > 0, \\ 0 & \text{if } i_{rf}(t) \le 0, \end{cases} \\ = V_D(t) \times SW^+(t), \tag{9}$$

where, $SW^+(t)$ is a square wave defined as,

$$SW^+(t) = \begin{cases} 1 & \text{if } i_{rf}(t) > 0, \\ 0 & \text{if } i_{rf}(t) \le 0. \end{cases} \tag{10}$$

Substituting from (5),

$$SW^+(t) = \begin{cases} 1 & \text{if } \Big[\cos(\omega_0 - \Delta\omega)t + \cos(\omega_0 + \Delta\omega)t\Big] > 0, \\ 0 & \text{otherwise.} \end{cases} \tag{11}$$

Noting that,

$$\cos(\omega_0 - \Delta\omega)t + \cos(\omega_0 + \Delta\omega)t = 2\cos\Delta\omega t \cos\omega_0 t, \tag{12}$$

the threshold condition of (11) is satisfied when $\cos\Delta\omega t$ and $\cos\omega_0 t$ are either both positive or both negative. Consider another periodic square wave with angular frequency ω, defined as,

$$\Pi_\omega(t) = \begin{cases} 1 & -\pi/2 \le \omega t \le \pi/2 \\ -1 & \pi/2 \le \omega t \le 3\pi/2. \end{cases} \\ = \frac{4}{\pi}\big(\cos\omega t - \frac{1}{3}\cos 3\omega t + \frac{1}{5}\cos 5\omega t - ...\big) \tag{13}$$

Note that $\Pi_\omega(t)$ has the same sign as $\cos\omega t$, and, hence, $\Pi_{\Delta\omega}(t)\Pi_{\omega_0}(t)$ has the same sign as $\cos\Delta\omega t\cos\omega_0 t$. Thus,

$$\Pi_{\Delta\omega}(t)\Pi_{\omega_0}(t) \quad = \begin{cases} 1 & \cos\Delta\omega t\cos\omega_0 t > 0 \\ -1 & \cos\Delta\omega t\cos\omega_0 t < 0 \end{cases} \tag{14}$$

From (11), (12) and (14), we conclude that

$$SW^+(t) = \frac{1}{2}\Big\{1 + \Pi_{\Delta\omega}(t)\Pi_{\omega_0}(t)\Big\}. \tag{15}$$

Thus, the nonlinearity contribution due to the positive excursion of $i_{rf}(t)$ is,

$$V_D^+(t) = \sum_{n=1}^{3} b_n A\Big[\cos(\omega_0 - \Delta\omega)t + \cos(\omega_0 + \Delta\omega)t\Big]^n \\ \times \frac{1}{2}\Big\{1 + SW_{\Delta\omega}(t)SW_{\omega_0}(t)\Big\} \tag{16}$$

The fundamental and the third-order intermodulation distortion (IMD_3) components can be calculated from the coefficients of $\cos(\omega_0 \pm \Delta\omega)t$ and $\cos(\omega_0 \pm 3\Delta\omega)t$ respectively in (16), i.e.

$$V_{1_D}^+(\omega_0 \pm \Delta\omega) = \frac{1}{2}b_1 A \tag{17a}$$

$$V_{3_D}^+(\omega_0 \pm 3\Delta\omega) = \frac{64}{45\pi^2}b_2 A^2 + \frac{3}{8}b_3 A^3 \tag{17b}$$

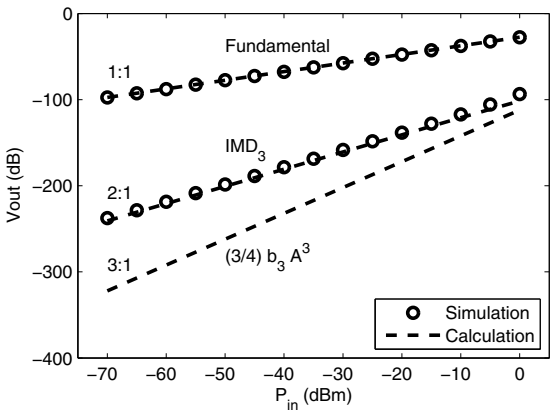

Fig. 4. Comparison between simulated (using BSIM3v3 model) and calculated (from (20) fundamental and third-order distortion signals for a CMOS passive mixer driven by a square LO with input and output terminals biased at 0 V. P_{in} is the input power of the LNA with ($g_{m,LNA}$ = 30 mS) in Fig. 3(a). The mixer source and load impedances are 500 Ω and 5 Ω respectively and LO frequency is 1 MHz. The simulated third-order distortion has a predominant 2:1 slope. For comparison, the calculated third-order distortion from (20) with slope of 3:1 is also plotted.

A similar analysis can be conducted for the negative half, and

$$V_D^-(\omega_0 \pm \Delta\omega) = \frac{1}{2}b_1' A \tag{18a}$$

$$V_D^-(\omega_0 \pm 3\Delta\omega) = -\frac{64}{45\pi^2}b_2' A^2 + \frac{3}{8}b_3' A^3 \tag{18b}$$

The combined fundamental and IMD_3 terms are obtained by combining (17) and (18), i.e.

$$V_D(\omega_0 \pm \Delta\omega) \approx \frac{1}{2}(b_1 + b_1')A \tag{19a}$$

$$V_D(\omega_0 \pm 3\Delta\omega) \approx \frac{64}{45\pi^2}(b_2 - b_2')A^2 + \frac{3}{8}(b_3 + b_3')A^3. \tag{19b}$$

Owing to the discontinuity in the second-order derivatives, the third-order intermodulation distortion becomes,

$$V_D(\omega_0 \pm 3\Delta\omega) \approx \frac{128}{45\pi^2}b_2 A^2 + \frac{3}{4}b_3 A^3. \tag{20}$$

The BSIM5 and PSP models use a single equation to define I_D in all regions, hence the coefficients are same in either region. Thus, in these cases

$$V_D(\omega_0 \pm 3\Delta\omega) = \frac{3}{4}b_3 A^3. \tag{21}$$

Eq. (20) reveals the contribution of the second-order nonlinearity to the third-order distortion. Fig. 4 shows the simulated (using BSIM3v3 model) and the calculated (from (19)) values for the fundamental and the third-order distortion of a passive mixer, demonstrating excellent agreement. At lower power levels, the second-order nonlinearity dominates IMD_3 simulation giving it a 2:1 slope with the input power. For comparison, the third-order term, $(3/4)b_3A^3$, from (21), with a 3:1 slope is also plotted.

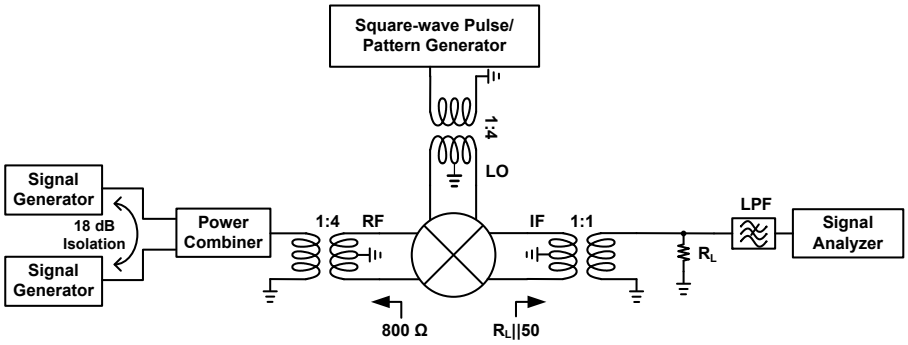

Fig. 5. Passive mixer measurement setup.

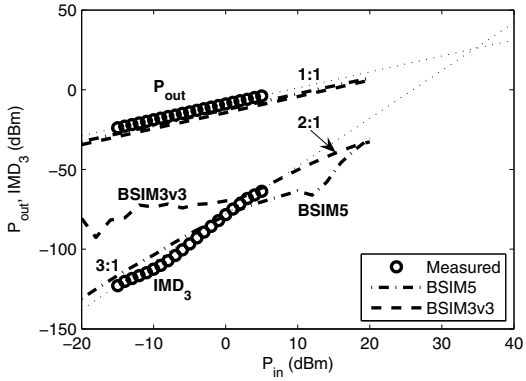

Fig. 6. Measured and simulated (SpectreRF) fundamental and IMD_3 curves for the passive mixer with +15 dBm sinusoidal LO at 500 MHz. The downconverted fundamental tones were measured at 20 MHz and the third-order intermodulation distortion tone was measured at 500 kHz.

IV. Measurement Results

Measurements were conducted to verify these calculations with a double balanced passive MOSFET mixer fabricated in a CMOS Silicon-on-Insulator (SOI) technology [13]. This technology uses an insulating substrate, which reduces the substrate losses and improves device performance.

Fig. 5 shows the measurement setup. The RF balun has a 1:4 turn ratio, which provides a high source impedance to the mixer. The two-tone spacing of 19.5 MHz was chosen to provide sufficient isolation and to minimize cross-talk between the signal generators. A low-pass filter is placed at the IF port to reject high-frequency signals. Fig. 6 shows the measured fundamental and IMD_3 curves for the passive MOSFET mixer driven by +15 dBm sinusoidal LO at 500 MHz. The measurement and simulations with BSIM5 model are in good agreement and have 3:1 slope for IMD_3, while, simulations with the BSIM3v3 model have a 2:1 slope for IMD_3 at higher power levels.

V. Conclusion

The linearity of a CMOS passive mixer was analyzed. In some models, the discontinuity in the second-order derivative of the drain-current leads to an erroneous slope of 2:1 for the third-order distortion. The mechanism behind this 2:1 slope was precisely identified. A passive mixer was measured to confirm the slope of 3:1 for IMD_3, and excellent agreement between theory and measurement was obtained.

Acknowledgement

The authors would like to acknowledge valuable discussions with Professors Gabriel Rebeiz and Peter Asbeck at UCSD, Mr. Don Kimball of the California Institute of Telecommunications and Information Technology at UCSD, and, Dr. Stephen Maas of Nonlinear Technologies Inc. The authors gratefully acknowledge Mr. Brain Hurst at Peregrine Semiconductors for providing experimental support. The authors acknowledge the support of the UCSD Center for Wireless Communications and its Member Companies, as well as a UC Discovery Grant.

References

[1] D. Manstretta and F. Svelto, "Analysis and optimization of IIP2 in CMOS direct down-converters," in *Proc. IEEE CICC*, 2002, pp. 243–246.

[2] M. Lehne, J. Stonick, and U. Moon, "An adaptive offset cancellation mixer for direct conversion receivers in 2.4GHz CMOS," in *Proc. IEEE Int. Symp. Circuits Syst.*, vol. 1, 2000, pp. 319–322.

[3] S. Zhou and M.-C. Chang, "A CMOS passive mixer with low flicker noise for low-power direct-conversion receiver," *IEEE J. Solid-State Circuits*, vol. 40, no. 5, pp. 1084–1093, May 2005.

[4] K. Joardar, K. K. Gullapalli, C. C. McAndrew, M. E. Burnham, and A. Wild, "An improved MOSFET model for circuit simulation," *IEEE Trans. Electron Devices*, vol. 45, no. 1, pp. 134–148, Jan. 1998.

[5] Bsim. [Online]. Available: http://www-device.eecs.berkeley.edu/~bsim3

[6] EKV Model. [Online]. Available: http://legwww.epfl.ch/ekv/

[7] N. D. Arora, R. Rios, C.-L. Huang, and K. Raol, "PCIM: a physically based continuous short-channel IGFET model for circuit simulation," *IEEE Trans. Electron Devices*, vol. 41, no. 6, pp. 988–997, June 1994.

[8] P. Bendix, P. Rakers, P. Wagh, L. Lemaitre, W. Grabinski, C. C. McAndrew, X. Gu, and G. Gildenblat, "RF distortion analysis with compact MOSFET models," in *Proc. IEEE CICC*, 3–6 Oct. 2004, pp. 9–12.

[9] G. Gildenblat, X. Li, W. Wu, H. Wang, A. Jha, R. Van Langevelde, G. D. J. Smit, A. J. Scholten, and D. B. M. Klaassen, "PSP: An advanced surface-potential-based MOSFET model for circuit simulation," *IEEE Trans. Electron Devices*, vol. 53, no. 9, pp. 1979–1993, Sept. 2006.

[10] X. J. Xi, J. He, M. Dunga, H. Wan, M. Chan, C.-H. Lin, B. Heydari, A. M. Niknejad, and C. Hu, "BSIM5 MOSFET model," in *Proc. IEEE Int. Conf. Solid-State IC Tech.*, vol. 2, 18–21 Oct. 2004, pp. 920–923.

[11] J. He, J. Xi, M. Chan, H. Wan, M. Dunga, B. Heydari, A. M. Niknejad, and C. Hu, "Charge-based core and the model architecture of BSIM5," 21–23 March 2005, pp. 96–101.

[12] S. A. Maas, "Two-tone intermodulation in diode mixers," *IEEE Trans. Microwave Theory Tech.*, vol. 35, no. 3, pp. 307–314, Mar 1987.

[13] P4140 Ultra-High Linearity Broadband Quad UltraCMOS(TM) FET Array. [Online]. Available: http://www.psemi.com/content/products/broadband/broadband_pe4140.html